All wavelengths and directions hybrid-guidance photonic crystal fiber and its property of Bragg grating resonance

Huijia Zhang,[1,2] Shuguang Li,[1,*] Chi Wah Leung,[2] and Helen Lai Wa Chan[2]

[1]State Key Laboratory of Metastable Materials Science and Technology, College of Science, Yanshan University, Qinhuangdao 066004, China

[2]Department of Applied Physics and Materials Research Centre, Hong Kong Polytechnic University, Hung Hom, Kowloon, Hong Kong, China

*Corresponding author: shuguangli@ysu.edu.cn

We propose a hybrid-guidance photonic crystal fiber (HG-PCF) that can guide light by the simultaneous effect of index guidance and photonic bandgap guidance at all wavelengths and directions. Index guidance is the dominant guidance mechanism at short wavelengths and photonic bandgap guidance is the dominant guidance mechanism at long wavelengths. The transmission spectrum of the Bragg grating in such a HG-PCF is also investigated.   © 2009 Optical Society of America

OCIS codes: 060.5295, 060.4005, 060.3735.

1. Introduction

Photonic crystal fibers (PCFs) consisting of airholes running down their lengths have been the subject of much interest in recent years. It has been demonstrated that PCFs guide light by two different mechanisms: index-guiding and photonic bandgap guiding [1]. Index-guiding PCFs have a core region of higher refractive index than the cladding, and lights are guided by a mechanism similar to step-index fibers. Photonic bandgap guiding arises from coherent Bragg scattering from the periodic arrangement of cylinders surrounding the core region, which may be a large air core or a material of lower refractive index than the surrounding medium. Although some of the most spectacular properties of photonic bandgap fibers (PBGFs) are found in hollow PCFs [1], photonic bandgap guidance can also be observed in silica core PCFs [2–5].

The silica-core PCFs (SC-PCFs) with high-index inclusion can support modes confined to the low-index core. These SC-PCFs have discrete and descending effective index curves as functions of the wavelength. These SC-PCFs have discrete bands of high and low transmission [2], which is typically a signature of photonic bandgap guidance. These spectacular features can be explained by the antiresonant reflecting optical waveguide (ARROW) model [6]. According to the ARROW model, the high-index inclusion in the cladding allows light to leak out from the core if they are on resonance, but reflects it back into the core if they are antiresonant.

Cerqueira et al. presented a hybrid-guidance PCF (HG-PCF) that can guide light by modified total internal reflection (TIR) and antiresonant reflection simultaneously [7]. The HG-PCF has shown that light confinement could occur through different mechanisms (TIR or ARROW guiding) depending on the direction, at a given wavelength. Such a HG-PCF is composed of airholes and Ge-doped silica rods disposed around an undoped silica core: the airholes are arranged in a hexagonal pattern as in an index-guiding PCF, while the high-index rods replace a single row of airholes along one of the PCF axes. Perrin et al. have presented a solid-core PBGF with

interstitial airholes (SC-PBGFIH) that makes TIR and bandgap modes coexist [8].

We propose a novel HG-PCF that can guide light simultaneously by index guidance and photonic bandgap guidance at all wavelengths and directions. Index guidance is the dominant guidance mechanism at short wavelengths and photonic bandgap guidance is the dominant guidance mechanism at long wavelengths.

2. All Directions and Wavelengths Hybrid-Guidance Photonic Crystal Fiber

The all directions and wavelengths HG-PCF is shown in Fig. 1. The square region is background silica. The outer solid circles represent high-index Ge-doped rods and the central dot is the Ge-doped core. The Ge-doped rods have a diameter of $d = 4.4\,\mu$m and a pitch of $\Lambda = 11\,\mu$m, whereas the Ge-doped core has a diameter of $d = 3\,\mu$m and $n_{si} = 1.444$. The relative refractive index difference between the Ge-doped high-index rods and silica is 1%, and the relative refractive index difference between the Ge-doped core and pure silica is 0.5%. The region inside the black circle, except the Ge-doped core, is the inner cladding.

The fundamental core modes and the bandgap map of the fiber are calculated by the finite element method and the plane wave expansion method, respectively, and the results are plotted in Fig. 2. Material dispersion of pure and doped silica have not been taken into consideration, but the calculated results for transmission windows and index contrasts will not be affected [9]. The curve indicating the effective refractive index curve of the fundamental core mode is labeled "Core modes." The fundamental core modes are located in the bandgap no matter if it is above the silica line or below the silica line. So bandgap guidance always affects the fundamental core modes of the fiber at all directions and wavelengths. Index guidance from the index contrast between the core and the inner cladding always affects the fundamental core modes of the fiber at all directions and
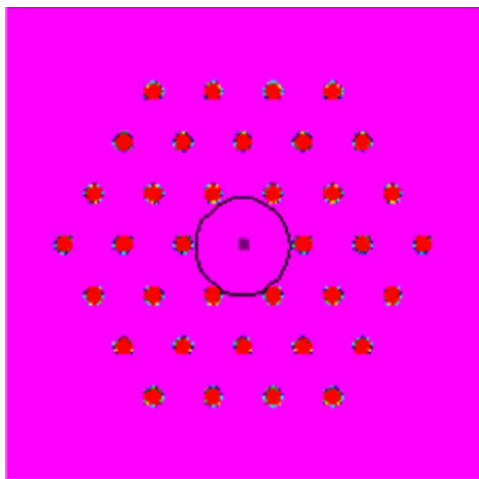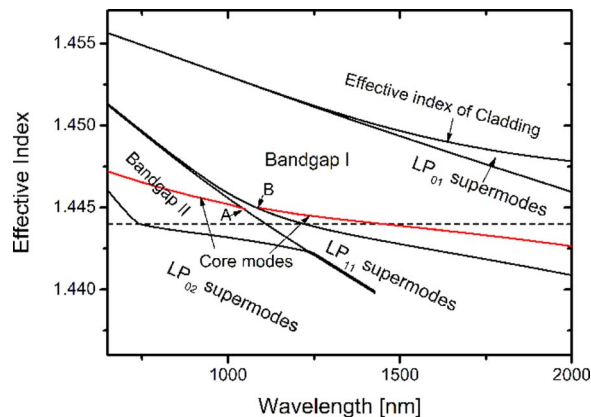
Fig. 2. (Color online) Fundamental core modes and bandgap map of the HG-PCF. The effective refractive index curve of the fundamental core modes is labeled "Core modes." Points A and B correspond to 1050 and 1090 nm, respectively.

wavelengths, also, so this fiber is a HG-PCF at all directions and wavelengths. The section of the core modes curve that is above the silica line is the index-guidance dominant region, because the fundamental core mode index of the fiber is higher than the silica index. The section of core modes curve that is below the silica line is the bandgap-guidance dominant region, because the fundamental mode index of the fiber is lower than the silica index. The transition point between the index-guidance dominant region and the photonic-bandgap-guidance dominant region is the intersection of the fundamental mode index curve and the silica line at $\lambda = 1450$ nm. The fundamental mode index curve on the silica line is broken at point A (1050 nm) and point B (1090 nm), because the fundamental core mode index and the LP_{11} supermode index of the high-index Ge-doped rods are equal between 1050 and 1090 nm. The energy of the fundamental core mode is coupled to the LP_{11} supermode of the high-index Ge-doped rods between 1050 and 1090 nm, so the loss of fundamental core mode is large between 1050 and 1090 nm. Further explanation about such a coupling effect was discussed by Lavoute et al. [10]. However, a loss peak will not be detected if we measure the transmission spectrum of the fiber between 1050 and 1090 nm, because the LP_{11} supermode of the high-index Ge-doped rods is a guided mode whose index is higher than the silica index. We will measure light guided by the LP_{11} supermode of high-index Ge-doped rods between 1050 and 1090 nm.

The results above can be explained by the special structure of the HG-PCF. It is believed that the inner cladding performs an important function for hybrid-guidance formation in the fiber. At short wavelengths, the modal field is small and is tightly confined around the Ge-doped core [Fig. 3(a)] since the Ge-doped core index is higher than the index of the pure silica in the inner cladding. The mode field is far from the first layer of high-index Ge-doped rods and, hence, the influence of the high-index Ge-doped rods on the modal field is weak. Index guidance is

Fig. 1. (Color online) Cross section of all directions and wavelengths HG-PCF.
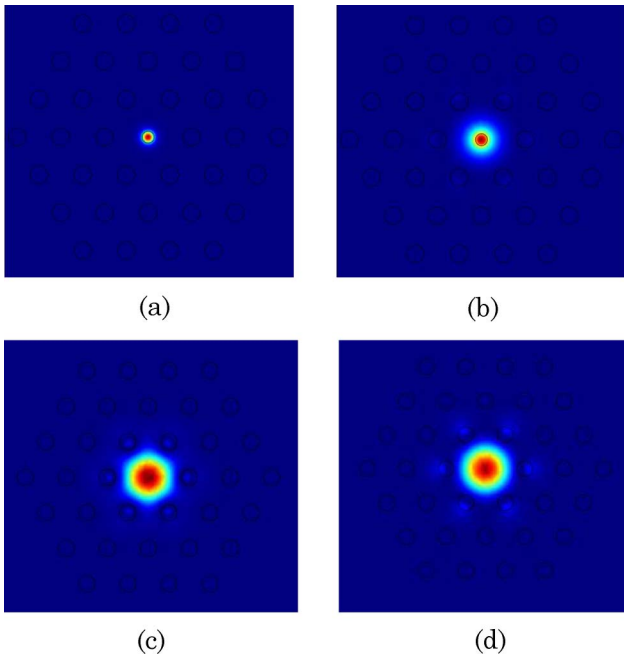
Fig. 3. (Color online) Mode field profiles: (a) and (b) HG-PCF at $\lambda = 900$ and 1650 nm, respectively; (c) and (d) HI-PCFP at $\lambda = 900$ and 1650 nm, respectively.

therefore the dominant guidance mechanism at short wavelengths. At long wavelengths, the modal profile spreads over a large region from the core [Fig. 3(b)]. Hence the influence of high-index inclusion on the modal field is strong. Photonic-bandgap guidance then becomes the dominant guidance mechanism at long wavelengths.

To further confirm that, Figs. 3(c) and 3(d) show modal profiles at short and long wavelengths in the high-index Ge-doped rod PCFs but with a pure silica core (HI-PCFP) instead of a Ge-doped core. Figures 3(b)–3(d) all show hexagonal modal profiles. The hexagonal modal profile shows the influence of the hexagonal arrangement of high-index rods on the modal field. Comparing Figs. 3(a) and 3(c), the modal profile of the HG-PCF at short wavelengths is circular, showing the influence of the circular Ge-doped

core. Moreover, the effective modal area of the HG-PCF is smaller than the HI-PCFP; hence the HG-PCF is easier to couple with single-mode fibers.

3. Property of the Bragg grating in the Hybrid-Guidance Photonic Crystal Fiber

Since the HG-PCF has a Ge-doped core and rods, a Bragg grating can be written in the HG-PCF. The transmission coefficient at the resonant peak in the fiber Bragg grating (FBG) is given by $T = 1 - \tanh^2(kL)$, where coupling coefficient k is usually used to measure the coupling strength between two modes. The coupling coefficient is determined by the overlap integral over the grating region as

$$k = \frac{\pi}{\lambda} \int\limits_{\text{grating}} E_i(x,y)E_j^*(x,y)\Delta n(x,y) \mathrm{d}x\mathrm{d}y. \quad (1)$$

Equation (1) suggests that one can calculate the coupling strength of mode resonances in a HG-PCF by calculating the overlap integral over the Ge-doped core and rod. However, since the energy portion in the six rods of the first layer surrounding the core is much higher than the other rods, the overlap almost entirely takes place over the core and these six rods. As a result, we can calculate the overlap integral with the core and six-rod supermode for simplification. The modes of the six-rod system can be considered as a linear combination of six orthonormal supermodes with a specific phase relation [11]. The phase difference between two adjacent rods is $\Delta\varphi = 2\pi n/6$ with $n = 0, \ldots, 5$. Nonzero overlaps are produced only when $n = 0, 2, 4$ [9], which is decided by the symmetry of the phase relationships, regardless of the modal profile in the rods. When $n = 0, 2, 4$, the LP_{01} supermode profiles are plotted in Fig. 4 and LP_{11} supermode profiles are plotted in Fig. 5. In Fig. 5(d), the modes with all the rod modes antisymmetrical about a radial line from the center of the microstructure cause zero overlap.

The computed transmission spectrum of the Bragg grating in a HG-PCF is shown in Fig. 6. The index modulation $\Delta n = 3 \times 10^{-4}$. The length of the grating
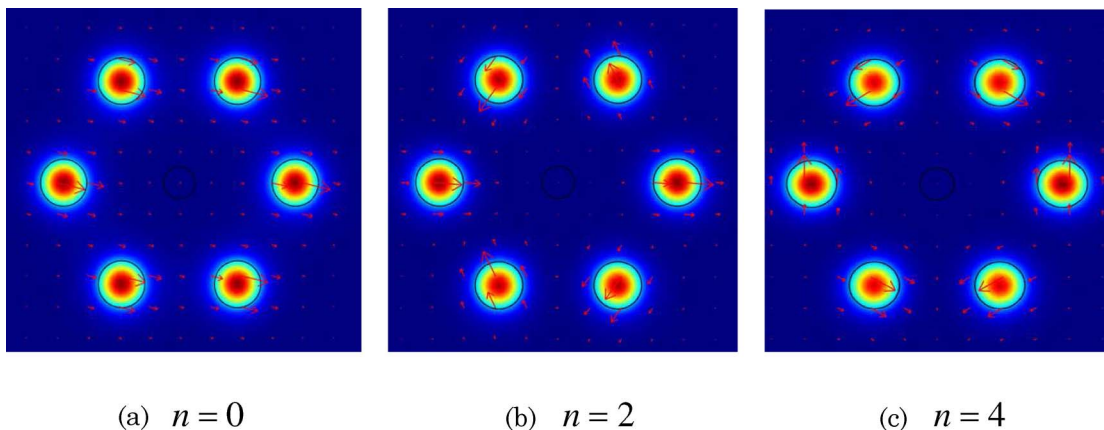

(a) $n = 0$ (b) $n = 2$ (c) $n = 4$

Fig. 4. (Color online) Modal profiles of the LP_{01} supermodes, which produce nonzero overlap. The amplitudes and directions of electric fields are represented by the arrows.
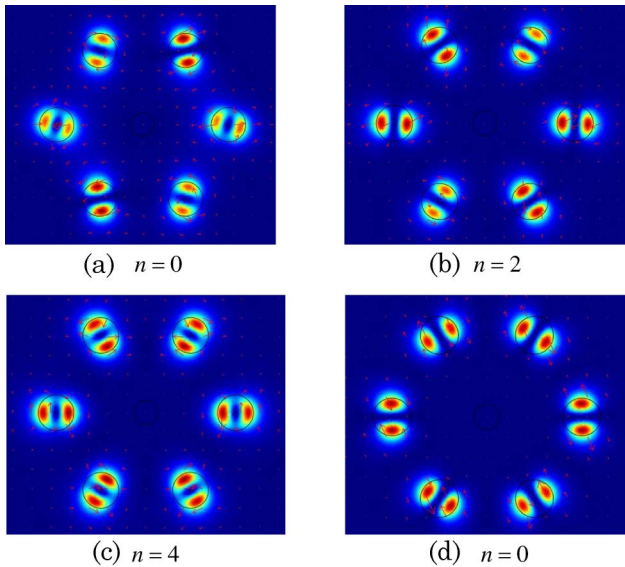
Fig. 5. (Color online) Some modal profiles of the LP_{11} supermode: (a), (b), and (c) can produce nonzero overlaps; (d) can produce zero overlaps.

Fig. 6. (Color online) Transmission spectrum of the Bragg grating in the HG-PCF: (a) $\Lambda_{FBG} = 311.3$ nm and (b) $\Lambda_{FBG} = 571.5$ nm.

region is 1.5 cm. The periods of grating are 311.3 and 571.5 nm in Figs. 6(a) and 6(b), respectively. In Fig. 6(a), when the period of grating is 311.3 nm, the main resonance wavelength is 900 nm. There is only one obvious resonant peak in the transmission spectrum of the FBG; it is formed by forward and backward fundamental core modes. The other resonant peak is formed by fundamental core mode and LP_{11} supermodes, but it is negligibly small as compared with the resonant peak formed by fundamental mode. When the period of grating is 571.5 nm, the main resonance wavelength is 1650 nm. There are multiresonant peaks in the transmission spectrum of the FBG. The larger resonant peak is formed by forward and backward fundamental core modes. The three smaller resonant peaks are formed by the fundamental core mode and the LP_{01} supermode. These results can be explained as follows. According to phase-match conditions $\lambda_B = 2n_{core}\Lambda_{FBG}$ and $\lambda_i = (n_{core} + n_{clad,i})\Lambda_{FBG}$, the resonant wavelength is short when the period of grating is small. The short resonant wavelength is in the index-guidance dominant region. The modal profiles of the fundamental core mode in the HG-PCF is small in the index-guidance dominant region and is tightly confined around the Ge-doped core, so the overlap between the fundamental core mode and the LP_{01}, LP_{11} supermode is small. There is only one obvious resonant peak formed by forward and backward fundamental core modes in the transmission spectrum of the FBG. On the other hand, the resonant wavelength is long when the period of grating is long. The long resonant wavelength is in the bandgap guidance dominant region. The modal profile of the fundamental core mode of the HG-PCF in the bandgap-guidance dominant region is spread out, with some energy diffusing into the six rods of the first layer. So the overlap of the fundamental core mode and the LP_{01} supermode is large.
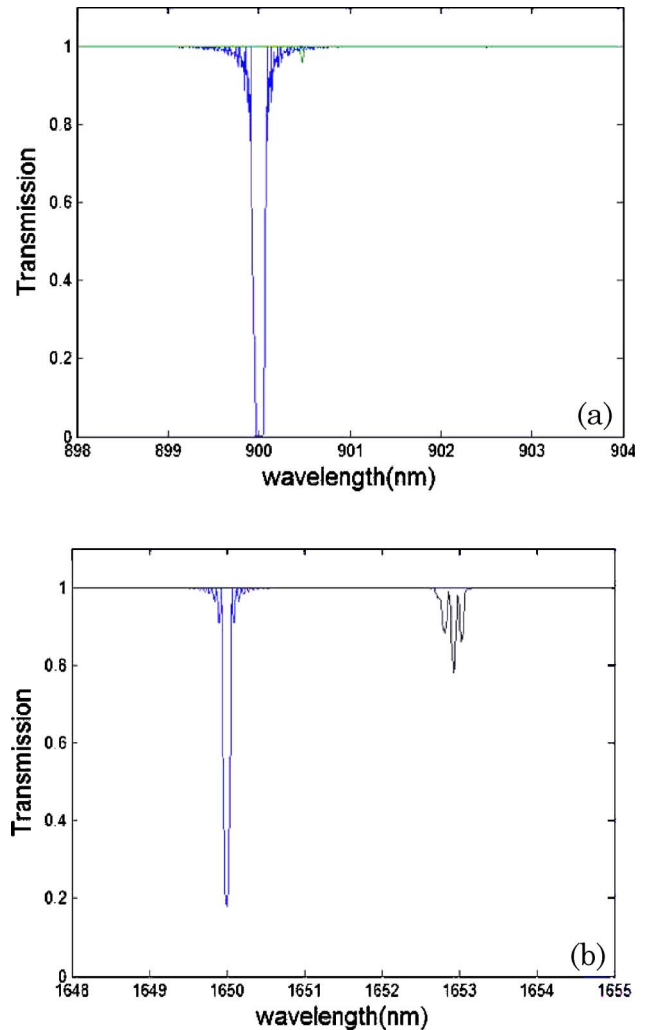
But the LP_{11} supermode is a lossy mode in the bandgap-guidance dominant region (the effective index curve of the LP_{11} supermode is under the silica line), so the overlap of the fundamental core mode and the LP_{11} supermode is small. This explains the occurrence of one main resonant peak formed by the forward and backward fundamental core modes and three smaller resonant peaks formed by the fundamental core mode and the LP_{01} supermode.

When the period of grating is $\Lambda_{FBG} = 346$ nm and the other parameters of the FBG are the same as the case in Fig. 6, the computed transmission spectrum of the FBG in HG-PCF is shown in Fig. 7(a). The larger main resonant peak is formed by the forward and backward fundamental core modes. The smaller resonant peak near the main resonant peak is formed by the fundamental core mode and the LP_{11} supermode. The peak at the right, which is negligibly small, is formed by the fundamental core mode and the LP_{01} supermode. The middle resonant peak formed by the fundamental core mode and the LP_{11} supermode in the index guidance dominant region, on the other hand, is obvious in the transmission

(a)
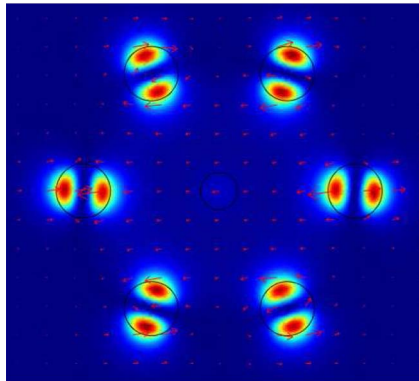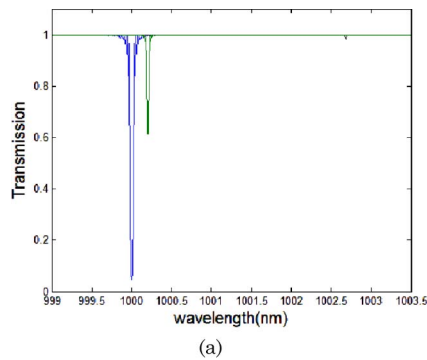
(b) $n = 0$

Fig. 7. (Color online) (a) Transmission spectrum of the Bragg grating in the HG-PCF when $\Lambda_{\text{FBG}} = 346\,\text{nm}$. (b) Modal profile of the LP_{11} supermode at 1000 nm when $n = 0$.

spectrum of the FBG. It can be explained as follows. The guided fundamental core mode at 1000 nm is near the edge of the bandgap and the effective index of the guided fundamental core mode is near the LP_{11} supermode (these results are found in Fig. 2). So some energy is coupled from the LP_{11} supermode in the first layer's six rods into the core region. In the modal profile of the LP_{11} supermode at 1000 nm in Fig. 7(b), at which $n = 0$, some energy has been coupled into the core region. When $n = 0$, the electrical field directions of the first layer's six rods are consistent, so the energy coupled into the core region from the six rods can be superposed with maximum amplitude. The overlap of the fundamental core mode and the LP_{11} supermode when $n = 0$ will be large. When $n = 2$ and 4, the electrical field directions of the first layer's six rods are not consistent, so the energy coupled into core region from different rods can be counteracted. The overlap of the fundamental core mode and the LP_{11} supermode when $n = 2$ and 4 will be small. So the middle resonant peak is mainly formed by the fundamental core mode and the LP_{11} supermode when $n = 0$.

4. Conclusions

We have demonstrated a HG-PCF that can guide light by index guidance and photonic-bandgap guidance at all wavelengths and directions, simultaneously. Index guidance that is similar to the single- mode step-index fiber is a dominant guidance mechanism at short wavelengths, and photonic-bandgap guidance is a dominant guidance mechanism at long wavelengths. We have also studied the property of the Bragg grating in the HG-PCF. When the period of grating is short, the resonant wavelength is in the index-guidance dominant region, and the transmission spectrum of the FBG in the HG-PCF has only one main resonant peak. When the period of grating is long, the resonant wavelength is in the bandgap-guidance dominant region, and the transmission spectrum of the FBG in the HG-PCF has several resonant peaks. When the resonant wavelength is near the edge of the bandgap, the transmission spectrum of the FBG in the HG-PCF has more than one resonant peak. With the development of the HG-PCF, the FBG in the HG-PCF will find wide application in fiber sensing and fiber communications.

References

1. J. C. Knight, "Photonic crystal fibres," Nature **424**, 847–851 (2003).
2. T. P. White, R. C. McPhedran, C. Martjin de Sterke, N. M. Litchinitser, and B. J. Eggleton, "Resonance and scattering in microstructured optical fibers," Opt. Lett. **27**, 1977–1979 (2002).
3. N. M. Litchinitser, A. K. Abeeluck, C. Headley, and B. J. Eggleton, "Antiresonant reflecting photonic crystal optical waveguides," Opt. Lett. **27**, 1592–1594 (2002).
4. A. K. Abeeluck, N. M. Litchinitser, C. Headley, and B. J. Eggleton, "Analysis of spectral characteristics of photonic bandgap waveguides," Opt. Express **10**, 1320–1333 (2002).
5. N. M. Litchinitser, S. C. Dunn, B. Usner, B. J. Eggleton, T. P. White, R. C. McPhedran, and C. Martijn de Sterke, "Resonances in microstructured optical waveguides," Opt. Express **11**, 1243–1251 (2003).
6. M. A. Duguay, Y. Kukubun, T. L. Koch, and L. Pfeiffer, "Antiresonant reflecting optical waveguides in SiO_2 – Si multilayer structures," Appl. Phys. Lett. **49**, 13–15 (1986).
7. S. A. Cerqueira, Jr., F. Luan, C. M. B. Cordeiro, A. K. George, and J. C. Knight, "Hybrid photonic crystal fiber," Opt. Express **14**, 926–931 (2006).
8. M. Perrin, Y. Quiquempois, G. Bouwmans, and M. Douay, "Coexistence of total internal reflexion and bandgap modes in solid core photonic bandgap fibre with intersticial air holes," Opt. Express **15**, 13783–13795 (2007).
9. L. Jin, Z. Wang, Y. Liu, G. Kai, and X. Dong, "Ultraviolet-inscribed long period grating in all solid photonic bandgap fibers," Opt. Express **16**, 21119–21131 (2008).
10. L. Lavoute, P. Roy, A. Desfarges-Berthelemot, V. Kermene, and S. Fevrier, "Design of microstructured single-mode fiber combining large mode area and high rare earth ion concentration," Opt. Express **14**, 2994–2999 (2006).
11. L. Michaille, C. R. Bennett, D. M. Taylor, T. J. Shepherd, J. Broeng, H. R. Simonsen, and A. Petersson, "Phase locking and supermode selection in multicore photonic crystal fiber lasers with a large doped area," Opt. Lett. **30**, 1668–1670 (2005).